sustainability

MDPI

Article

Enrichment of Anammox Bacteria Using Anammox Sludge as a Primer Combined with Ordinary Activated Sludge

Lifang Liu [1,2], Meiling Hu [3], Cong Wang [1,2,*], Weikang Qi [1] and Yongzhen Peng [1]

[1] National Engineering Laboratory for Advanced Municipal Wastewater Treatment and Reuse Technology, Key Laboratory of Beijing for Water Quality Science and Water Environment Recovery Engineering, Beijing University of Technology, Beijing 100124, China; l1978659045@163.com (L.L.); qiweikang10@163.com (W.Q.); pyz@bjut.edu.cn (Y.P.)
[2] Beijing Drainage Group Co., Ltd., Beijing 100044, China
[3] D.smart Environmental Technology Co., Ltd., Beijing 100102, China; hook361@163.com
* Correspondence: 18001093291@163.com; Tel.: +86-180-0109-3291

Abstract: Anaerobic ammonia oxidation bacteria (AnAOB) are difficult to cultivate due to their long start-up time and sensitivity to environmental conditions. In this study, anammox granular sludge was cultured with ordinary activated sludge under influent dissolved oxygen concentrations of 6–8 mg/L, successfully enriching AnAOB. The presence of multiple microorganisms in the activated sludge enabled the anammox system to resist the unfavorable influent environment and sustain system stability. The total nitrogen removal rate reached a maximum of 81%, and the TN effective load increased from 0.1 to 1.5 kg $N/m^3/d$. The results showed that the dissolved oxygen present in the influent did not lead to a breakdown in the anammox system. The protein in the sludge extracellular polymeric substances played an important role in the enrichment of AnAOB, and the sludge settling performance at the bottom of the reactor was better than that at the top of the reactor, with protein/polysaccharide in the range of 5–6.3. *Candidatus brocadia* and *Candidatus kuenenia* were the main anammox functional bacteria in the system. On 153 d of reactor operation, their relative abundances were 8.51 and 5.68%, respectively. This study shows that microorganisms in activated sludge contribute to the stability of the anammox system when the influent conditions are appropriate. This provides a new idea for the rapid start-up of the anammox system and enrichment of AnAOB.

Keywords: anammox; activated sludge; granular sludge; nitrogen removal; microbial communities; extracellular polymeric substances

Citation: Liu, L.; Hu, M.; Wang, C.; Qi, W.; Peng, Y. Enrichment of Anammox Bacteria Using Anammox Sludge as a Primer Combined with Ordinary Activated Sludge. *Sustainability* **2023**, *15*, 12123. https://doi.org/10.3390/su151612123

Academic Editor: Saviour A. Umoren

Received: 11 June 2023
Revised: 6 August 2023
Accepted: 7 August 2023
Published: 8 August 2023

1. Introduction

Discharges of excessive quantities of nitrogen into water bodies lead to the disruption of aquatic ecosystems and to the eutrophication of water bodies [1]. However, with increasing industrialization in China, large quantities of factory wastewater are being discharged into wastewater treatment plants, and the carbon-to-nitrogen ratio of this wastewater is often not sufficient for traditional denitrification-driven nitrogen removal processes [2]. Many wastewater treatment plants face problems associated with the high cost of organic carbon addition and with meeting discharge standards [3]. In this context, new organic carbon-saving processes have been developed. The anaerobic ammonia oxidation (anammox) reaction allows for nitrogen removal without the consumption of organic carbon and aeration. This not only conserves carbon sources but also saves energy, and the approach has therefore gained attention [4]. However, several difficulties have been found in the study of anammox. One anammox reaction substrate is NO_2^--N, which is uncommon as an intermediate product in wastewater treatment [5]. To generate stable NO_2^--N as a substrate, two processes, partial nitrification, and partial denitrification, have been developed to achieve NO_2^--N accumulation [6–8]. In addition, it was found that anaerobic ammonia-oxidizing bacteria (AnAOB) are sensitive to environmental conditions

and have a long generation time (11–20 d), leading to a long start-up time [9]. These difficulties limit the large-scale application of anammox technology.

During the long start-up and in situ enrichment process of anammox systems, the systems have been reported to have nitrogen removal efficiencies much lower than the theoretical value [10,11]. Researchers have explored methods to reduce bacterial growth inhibition [12]. Fast start-up and granulation of anammox systems have been achieved by the addition of extracellular polymers [13], reduced graphene [9], and Fe(II) [14] and by the action of applied electric fields [15]. Zekker et al. used anaerobic and aerobic sludge as feed sludge and hydrazine to accelerate the start-up of the anammox system with a 110 d start-up time [16]. Another approach is to accelerate start-up by using anammox granular sludge as the seed sludge or biofilm [17]. In a previous study, researchers employed 3–15% AnAOB carriers along with new carriers to rapidly start up a single-stage deammonified moving bed biofilm reactor within a few months [18]. Wang et al. attempted to start the activated sludge as inoculum with a low concentration of anammox (0.2 g VSS/L) as seed sludge. The start-up time was greatly reduced, and the total nitrogen (TN) removal reached 70% [19].

AnAOB grow slowly and are not easily retained in suspended sludge obtained from ordinary activated sludge processes [20,21]. Liu et al. investigated the interaction matrix between suspended sludge and anammox biofilm. The results showed that the introduction of suspended sludge significantly reduced the nitrogen removal of anammox from 83.8 $\pm$ 6.5 to 48.7 $\pm$ 17.0% [20]. Zhao et al. realized a pure biofilm anammox process by continuously reducing the concentration of suspended sludge. The nitrogen removal efficiency increased from 62.1 $\pm$ 4.5 to 79.2 $\pm$ 3.9% [22]. Tao et al. investigated the effect of different seed sludge on AnAOB enrichment and concluded that the initial seed sludge had a uniform microbial community and that a high concentration of AnAOB was favorable for rapid start-up. He believed that the initiation strategy was more important and should retain significant microorganisms and eliminate unimportant microorganisms [23]. In summary, suspended sludge was thought to increase competition between denitrifying bacteria and AnAOB in the system (Table 1). However, the wide variety of microorganisms in activated sludge may be a favorable condition. When the influent conditions are suitable, it is possible to cancel the unfavorable environment entering the system, such as organic matter and dissolved oxygen (DO), with the help of a variety of microorganisms, thus providing a more suitable environment for the survival of AnAOB.

Previous studies showed that AnAOB are very sensitive to DO concentrations, and 5% oxygen saturation can cause inhibition of the anammox process, which would only occur when there was no DO in the environment. Furthermore, when AnAOB were in an environment with 18% oxygen saturation, complete inactivation occurred, which could not be recovered even if the DO was subsequently removed [24,25]. However, in practical engineering applications, some DO is typically present in wastewater entering the anammox process after the aerobic degradation of organic matter or after partial nitrification at the front end to obtain NO_2^--N. The effect of DO carried over from the previous process of nitrogen removal from the anammox system has not been specifically determined. Most existing studies start with the removal of DO present in the influent water [25], and there are fewer studies on the effect of DO carried over in the influent on anammox [26].

In conclusion, the main objective of this study was to investigate the effect of DO carried in the influent on anammox. Rapid enrichment of AnAOB was achieved by incubating waste sludge and anammox granular sludge with a 2:1 ratio. The microbial transformation was manifested through the combination of extracellular polymeric substances, sludge surface special, microbial community, and effluent water quality.

Table 1. Rapid enrichment AnAOB strategies and enhancement strategies.

Cultivation Strategy	Inf. NH_4^+-N	Inf. NO_2^--N	TN Removal Efficiency	NRR	Start-Up Time	References
	mg/L	mg/L	%	kg N/(m^3·d)	d	
Addition of extracellular polymeric substances.	60–200	80–250	-	0.05–0.75	19	[13]
Activated sludge as inoculum, fed with a low concentration of anammox sludge.	30–160	40–180	>70	-	5	[19]
Biochar accelerates start-up	140	140	80.0 ± 9.6	1.48	85	[27]
low frequency and intensity ultrasound.	70	70	86	0.68	53	[28]
Inoculating denitrifying granular sludge	50–220	50–300	-	0.72	28	[29]
mixed AnAOB inoculated with flocculent	75–210	75–230	-	0.5	73	[30]
nitritation sludge feed in ferrous iron.	50	50	-	0.16	50	[31]
Inoculating perchlorate reduction sludge and a small amount of anammox sludge.	200	200	73.20 ± 6.79%	-	41	[32]
A novel electrolysis-integrated anammox system	420	420	90.12–90.80	-	-	[33]
cultivation strategy	90–95	105–110	75.3	0.67	-	[34]

2. Materials and Methods

This paper was based on running an up-flow anaerobic sludge blanket (UASB) reactor for AnAOB enrichment. The specific materials and methods are as follows:

2.1. Experimental Setup and Operation Strategy

The UASB reactor used in the experiments had an effective volume of 4 L, an inner diameter of 0.07 m, and a height of 1.2 m and was made of Plexiglas (Figure S1). The top of the reactor was equipped with a three-phase separator. The uplifted sludge returned to the reactor by gravity; the gas reached upwards to the top and was collected. The inlet bucket of the reactor was a 40 L cylindrical tank. The influent was pumped into the bottom of the reactor from the inlet bucket by a peristaltic pump (Lange, Shijiazhuang, China), and the effluent water overflowed from the top of the reactor. Water from the upper part of the reactor was pumped through the peristaltic pump to the inlet pipe for reflux. The return flow rate was 100 L/d. The outer wall of the reactor was wrapped with a heating (JCS, Suzhou, China) and temperature-retention belt to control the temperature inside the reactor at 30 ± 1 °C (Figure S2).

The reactor was continuously fed and continuously discharged. The hydraulic retention time (HRT) was 17.4 h at the beginning and then gradually reduced to 2.2 h. At this time, the reactor sludge layer was approximately 500 mm from the outlet, and there was almost no sludge loss except for a small amount of flocculated mud. pH, DO, and temperature were monitored daily. NH_4^+-N, NO_2^--N, and NO_3^--N in the influent and effluent of the reactor were monitored regularly using standard methods [35].

2.2. Seed Sludge and Feed Wastewater

In this study, the inoculated sludge was anammox granular sludge and ordinary waste sludge in a 1:2 ratio. The particle size of the inoculated anammox sludge ranged from 10 to 2000 μm, with an average particle size between 350–400 μm. The average

particle size of activated sludge was less than 100 μm. The feed was synthetic wastewater made from nutrient-added recycled water. The recycled water contained approximately 5 mg/L NH_4^+-N and 10 mg/L NO_3^--N, and the DO concentration was 6–8 mg/L. Ammonium bicarbonate and sodium nitrite were used to provide the main influent NH_4^+-N and NO_2^--N with initial concentrations of 50 mg/L and 66 mg/L, respectively, and these concentrations were gradually increased thereafter. The mineral elements and trace elements required for microbial growth were also added to the influent.

2.3. Batch Test

The effect of substrate (NH_4^+-N, NO_2^--N, and COD) concentration on the anammox reaction was investigated using sludge incubated for approximately 200 d in the reactor. Equal amounts of sludge were placed in five 1 L conical flasks, the sludge was washed three times with oxygen-free distilled water, and then the volume was fixed to 1 L. The DO concentration of the sludge-water mixture in the flasks was ensured to be less than 0.1 mg/L.

For the effect of COD, 2.5, 5, 25, and 40 mL of sodium acetate concentrate (COD of 20 g/L) were added, respectively, while 1 mL of ammonium bicarbonate concentrate (NH_4^+-N of 23 g/L) and 1.32 mL of sodium nitrite concentrate (NO_2^--N of 23 g/L) were added. For the effect of NH_4^+-N, 1–5 mL of ammonium bicarbonate concentrate and 1 mL of sodium nitrite concentrate were added, respectively. For the effect of NO_2^--N, 1–5 mL of sodium nitrite concentrate and 1 mL of ammonium bicarbonate concentrate were added, respectively.

After adding the concentrate, stir quickly until well mixed, take 10 mL of mud-water mixture, and quickly centrifuge the supernatant. The measured NH_4^+-N and NO_2^--N values were the initial concentration values. Then, the bottles were quickly sealed and incubated in a constant temperature incubator at 31 °C. The substrate concentration was measured by taking samples every 2 h. pH of 8.0–8.5 for the whole process.

2.4. Extraction and Determination of Extracellular Polymeric Substances

Loosely bound extracellular polymeric substances (LB-EPS) and tightly bound extracellular polymeric substances (TB-EPS) were extracted using a modified thermal extraction method [36]. LB-EPS was extracted using a 0.5% NaCl solution at 70 °C, followed by TB-EPS in a water bath at 60 °C for 30 min. The protein (PN) and polysaccharide (PS) composition was determined. PN was determined by the Folin-Ciocalteu method. PS was determined by the phenol-sulfuric acid method [36].

2.5. Scanning Electron Microscopy Observations

The surface morphology of the sludge was observed using a GeminiSEM (Jena, Germany) 300 field emission scanning electron microscope. Sludge samples were fixed in glutaraldehyde (2.5%), rinsed in a phosphate-buffered solution, dehydrated in a gradient of ethanol (50%, 70%, 80%, 90%, and 100%), and dried after displacement. Finally, the samples were observed after the surface of the samples was coated with a metal film.

2.6. Microbial Analysis Methods

The sludge samples were centrifuged, and the supernatant was removed and lyophilized in a lyophilizer (LABCONCO, Kansas City, MO, USA). The lyophilized sludge was weighed to 0.1 g, and DNA was extracted using a Fast DNA spin kit (MP bio, Santa Ana, CA, USA). The extracted genomic DNA was then detected by 1% agarose gel electrophoresis and amplified using an ABI GeneAmp® 9700 PCR instrument. The 16S rRNA gene-specific amplification primers used were 338F and 806R. The samples were sent to Majorbio Group for high-throughput sequencing on an Illumina MiSeq platform after DNA extraction, monitoring, and amplification. The sequenced data were quality-controlled, screened, and partitioned to analyze their microbial communities at all levels.

3. Results and Discussion

Anammox granular sludge was mixed and incubated with ordinary waste sludge. The enrichment of AnAOB was further characterized by effluent quality, sludge EPS, microbial surface characteristics, and microbial community succession.

3.1. Nitrogen Removal Performance

The influent NH_4^+-N and NO_2^--N concentrations were 50 mg/L and 66 mg/L, respectively, at the beginning of the operation, and the HRT was 17.4 h (Figure 1). At this time, the effluent TN removal efficiency was 39.3%, and the TN effective load was only 0.13 kg N/m^3/d (Figure 2). There was no significant increase in the TN removal efficiency for 15 d, probably because the sludge was newly inoculated, had low activity, and needed time to adapt to the environment [19]. It was also found that there was a buildup of reactor sludge. After 16 d, the reflux was increased to achieve a reflux rate of 100 L/d, and the HRT was reduced to 10.2 h. Subsequently, the effluent NH_4^+-N and NO_2^--N continued to decrease to approximately 5 mg/L (Figure 1a,b), and the effluent NO_3^--N concentration increased from 10 to 17 mg/L (Figure 1c). Nutrients and sludge were in full contact, and microorganisms started to adapt to the environment. In this situation, the TN removal efficiency reached 79%, the TN effective load increased to 0.25 kg N/m^3/d, and the reactor was successfully initiated. The influent NH_4^+-N and NO_2^--N concentrations further increased to 80 and 105 mg/L, respectively, on 63 d. However, the effluent NH_4^+-N increased sharply to 22 mg/L, and NO_2^--N was 38 mg/L. The concentration did not decrease significantly for 15 d, and the average TN removal efficiency was 56%. When the influent TN concentration reached 200 mg/L, the nitrogen removal efficiency decreased significantly, and the anammox reaction was inhibited. In Wang et al.'s study, an increase in effluent substrate concentration was also observed when both influent NH_4^+-N and NO_2^--N concentrations were increased to 100 mg/L [29]. It has been suggested that this was due to inhibition caused by high nitrite concentrations [27]. It has been shown that a high substrate concentration stimulates microorganisms to secrete extracellular polymers rapidly, blocking gas-release channels and causing particle cleavage [37]. It has also been shown that free ammonia and free nitrite alter the cellular transmembrane potential, resulting in inhibition [38]. In conclusion, a high concentration of substrate inhibited AnAOB.

To reduce the inhibition effect of substrate concentration, the influent NH_4^+-N and NO_2^--N were adjusted to 65 and 85.8 mg/L on 81 d. After the substrate concentration was reduced, the effluent NH_4^+-N and NO_2^--N concentrations rapidly decreased to below 5 mg/L (Figure 1a,b). The TN removal rate recovered to 78% (Figure 2). This result indicates that when AnAOB are inhibited by a high substrate concentration, the inhibition can be mitigated by reducing the substrate amount. To further increase the load, the HRT gradually decreased from 6.4 to 2.2 h from 96 to 194 d (Figure 1c). Stable operation of the reactor was maintained, with an effluent NH_4^+-N below 2 mg/L and NO_2^--N of approximately 5 mg/L after 200 d. The removal rates of NH_4^+-N and NO_2^--N reached more than 95%, and the average effluent NO_3^--N was 26.8 mg/L. With the enrichment of AnAOB, the TN effective load increased from 0.1 to 1.5 kg N/m^3/d (Figure 2). This was not the maximum load that the reactor could achieve and continued increases in influent flow or concentration were expected to continue to increase its load. The TN removal rate was stable at approximately 80%, which was 8% lower than the theoretical anammox TN removal rate of 89% [39]. The 6–8 mg/L DO present in the influent converted 1–3 mg/L NH_4^+-N. Therefore, in the fitting results for the long-term experiment, the NO_2^--N to NH_4^+-N ratio was approximately 1.25 (Figure S3), which was slightly lower than the theoretical value of 1.32 [39], and the NO_3^--N to NH_4^+-N ratio was approximately 0.25, which was close to the theoretical value of 0.26 [39].

The anammox system cultivated in this study was a coexistence of suspended sludge and granular sludge. Zhao et al. achieved a pure biofilm anaerobic ammonia oxidation process by continuously reducing the concentration of suspended sludge. The nitrogen removal efficiency increased from 62.1 ± 4.5 to 79.2 ± 3.9% [22]. Its nitrogen

removal efficiency was not much different from this study. In contrast to studies starting with single nitrifying sludge, anaerobic activated sludge, etc. [23,31], the present study showed significant TN removal at the very beginning. Moreover, the high concentration of basal AnAOB resulted in more rapid microbial growth, which greatly saved time for reactor startup.

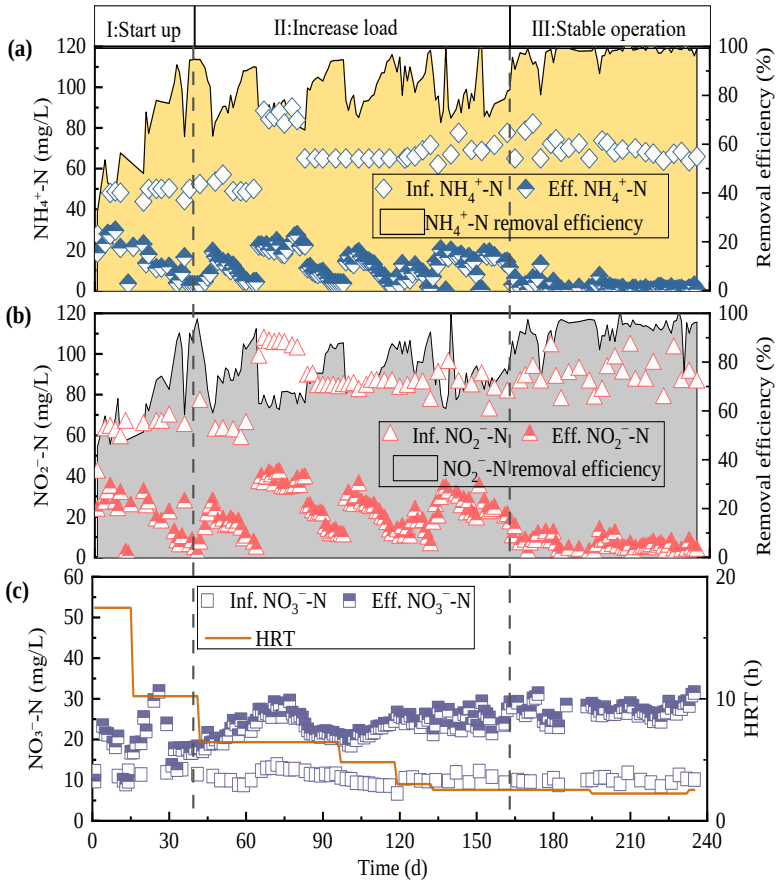

Figure 1. Nitrogen conversion in the anammox reactor. Influent and effluent NH_4^+-N (**a**); NO_2^--N (**b**) concentrations and removal efficiency; (**c**) influent and effluent NO_3^--N concentrations and HRT.

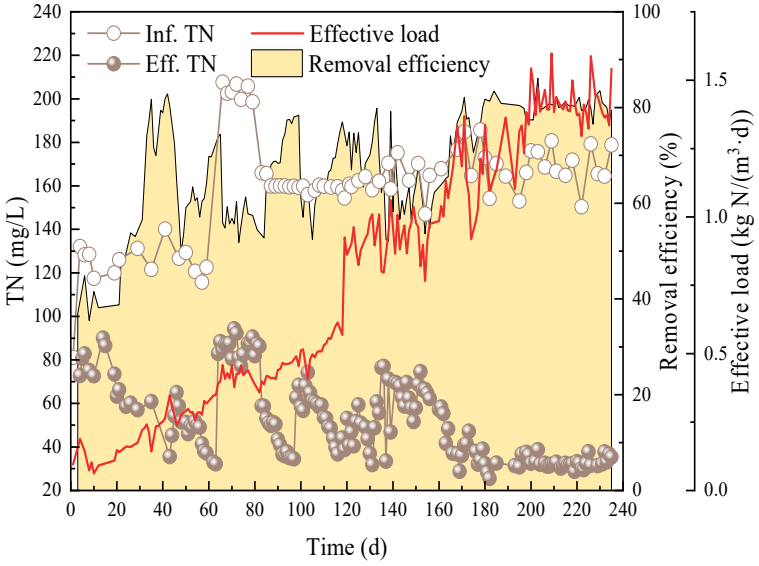

Figure 2. Influent and effluent TN concentration, TN removal efficiency, and TN effective load of the anammox reactor.

3.2. Changes in Sludge Extracellular Polymeric Substances

EPSs play a crucial role in promoting microbial coagulation and adhesion. Additionally, they contribute significantly to maintaining system stability and facilitating particle formation [40]. EPS was extracted from the sludge at different heights of the reactor and in different periods, and the PN and PS contents were determined for analysis.

Sludge at 10, 40, and 70 cm from the bottom was taken on 60 d of reactor operation. LB-EPS and TB-EPS were extracted, and Total-EPS was calculated as the sum of LB-EPS and TB-EPS. The sludge mixed liquor volatile suspended solids concentrations were 17.16, 8.93, and 5.72 g/L from the bottom to the top of the reactor. Consistent with the findings of others [41], the PN content was greater than the PS content in EPS at different heights. The highest PS and PN contents were 1.43 and 4.54 mg/g VSS in LB-EPS and 5.30 and 27.53 mg/g VSS in TB-EPS, respectively. The PN/PS index showed a decreasing trend from the upper to the lower part of the reactor, with the PN/PS value of Total-EPS decreasing from 10.46 to 2.57. PS are hydrophilic substances, and a small amount of PS secretion is beneficial to adhesion between microorganisms. However, the secretion of higher amounts of PS increases sludge viscosity [42]; in contrast, PN and amino acid-like PN substances are reported to contain a high negative charge and are hydrophobic substances, which can promote cell aggregation and contribute to sludge-settling performance [43]. Therefore, a high content of PN in EPS helps to promote and maintain good sludge settling performance. In summary, the sludge in the lower part of the reactor had better settling performance.

The EPS of the sludge extracted at a 20 cm height was analyzed on 60, 130, and 240 d (Figure 3d–f). The sludge mixed liquor volatile suspended solids were 17.16, 23.1, and 19.93 g/L, respectively. As the reactor operated, the PS content remained relatively stable, whereas the PN content gradually increased, leading to a gradual increase in EPS within the sludge. The highest levels of PS in LB-EPS and TB-EPS were 2.71 and 8.87 mg/g VSS, and the highest levels of PN were 5.48 and 48.89 mg/g VSS, respectively. Similarly, the PN content was consistently greater than the PS content, and the total EPS content on 240 d was significantly higher than that prior to 130 d. The PN/PS results revealed that on both 60 and 130 d, the ratio ranged between 1.5 and 3.5. However, on 240 d, the ratio significantly increased to 5–6.3. This could be because the increase in load caused the microorganisms to secrete more EPS, while the increase in PN was more favorable for particle stabilization [44]. This indicates that the anammox sludge culture was more mature and had better sedimentation performance on 240 d.

The 60 and 130 d sludge EPS were subjected to three-dimensional excitation-emission matrix fluorescence spectroscopy to analyze the substances present, as shown in Figure S4. PN-like substances were detected in the sludge EPS, with two main types of peaks, one peak (peak 1) in the wavelength range of 220–230/305–340 and the other peak (peak 2) in the wavelength range of 275–285/330–340; peak 1 belongs to aromatic-like PN, and peak 2 is a soluble microbial byproduct corresponding to tryptophan-like substances [45]. Essentially, no PS were found. The results are consistent with the trends in the PN and PS contents in the EPS measured above. It also showed the importance of PN-like substances for microorganisms.

3.3. Sludge Surface Characteristics and Microbial Community Structure

Figure 4a,b show photographs of the sludge from the reactor after operation for 0 and 240 d. The domesticated sludge had a dark red color, and the granules exhibited a variety of shapes and sizes. This is probably related to the fact that the inoculated sludge consisted of flocculent-activated sludge and granular anammox sludge. The gradual change in the microorganisms present in the sludge during the domestication process may have also played a role [38]. The yellow-brown color of the activated sludge that was inoculated at the beginning was essentially no longer visible in the reactor, indicating that the microorganisms changed. Apparently, AnAOB had become the dominant bacteria. To further observe the surface properties of the sludge, the sludge at the bottom (10 cm height)

of the reactor on 240 d was observed by scanning electron microscope (SEM), and the results are shown in Figure 4c–e. The sludge contained dense material. At increased magnification, spherical and ellipsoidal microorganisms were observed, and the microorganisms were connected to each other by mesh-like substances (Figure 4d,e), presumably extracellular polymers secreted by the microorganisms [3]. A small number of other shapes, such as filamentous and rod-shaped microorganisms, were also observed, indicating the coexistence of other microorganisms. Other studies have also indicated that the anammox system is a result of the collective action of various microorganisms [46].

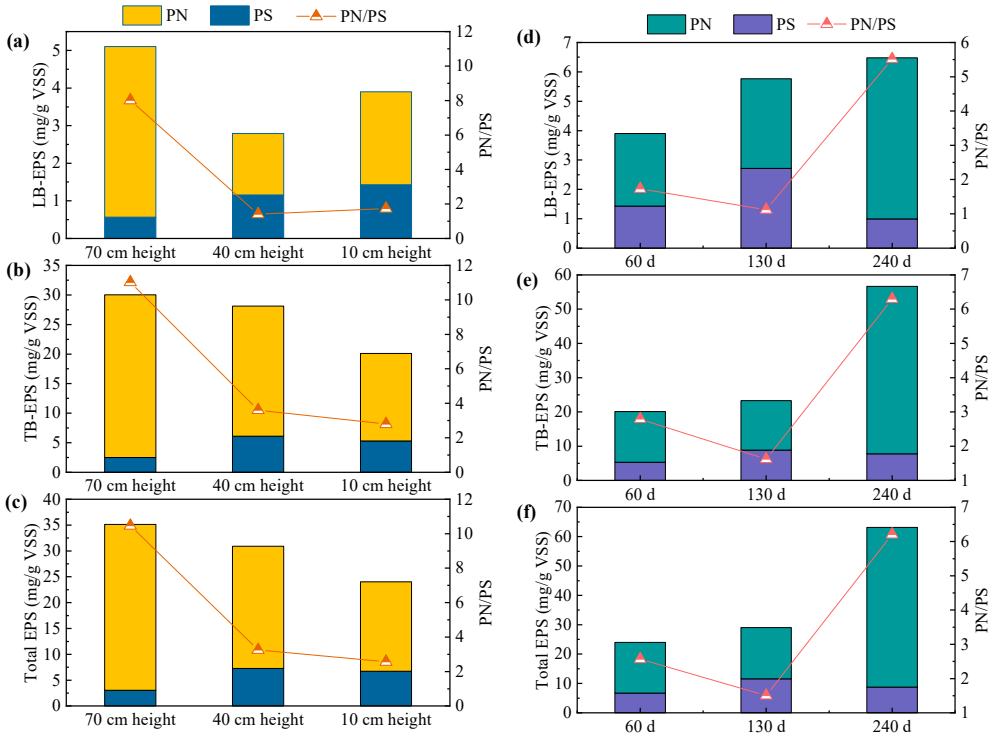

Figure 3. EPS indicators. (**a**–**c**) Sludge LB-EPS, TP-EPS, and Total-EPS at 10 cm height, 40 cm height, and 70 cm height in the UASB reactor after operation for 60 d. (**d**–**f**) Sludge EPS at 10 cm height in the UASB reactor after operation for 60, 130, and 240 d.

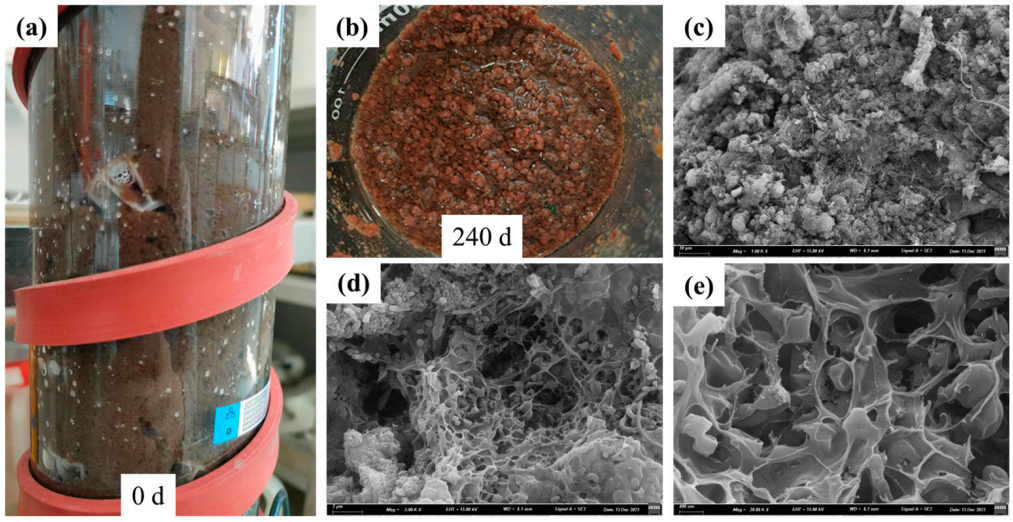

Figure 4. Reactor sludge phenological characteristics. (**a**) Photograph of inoculated sludge, (**b**) photographs of sludge after reactor operation for 240 d, (**c**–**e**) SEM images of sludge on 240 d.

Sludge samples from the reactor on 123 and 153 d of operation at 10 cm from the bottom were analyzed with high-throughput sequencing. The main bacterial phyla were *Chloroflexi* (52.31 and 73.24%), *Proteobacteria* (8.49 and 19.44%), *Planctomycetes*, *Bacteroidetes*, and *Acidobacteria* (Figure 5a). This finding aligns with previous reports on the majority of anammox systems [47,48]. *Chloroflexi* had the highest percentage in this study, and it was also found in a high percentage of many anammox systems [49]. *Chloroflexi* was reported to provide a stable skeleton for granular sludge formation along with cellular organic matter and metabolites of dead microorganisms [50]. During the conversion of sludge, the original microorganisms in the sludge gradually died and transformed, and the substances released into the system caused the proliferation of *Chloroflexi*. Combined with the conclusions of others, the high abundance of *Chloroflexi* favored the stability of the anammox system. AnAOB are mainly composed of *Proteobacteria*, which promote the enrichment of anaerobic AnAOB by producing secondary metabolites [48]. The percentage of Proteobacteria increased significantly with the operation of the reactor.

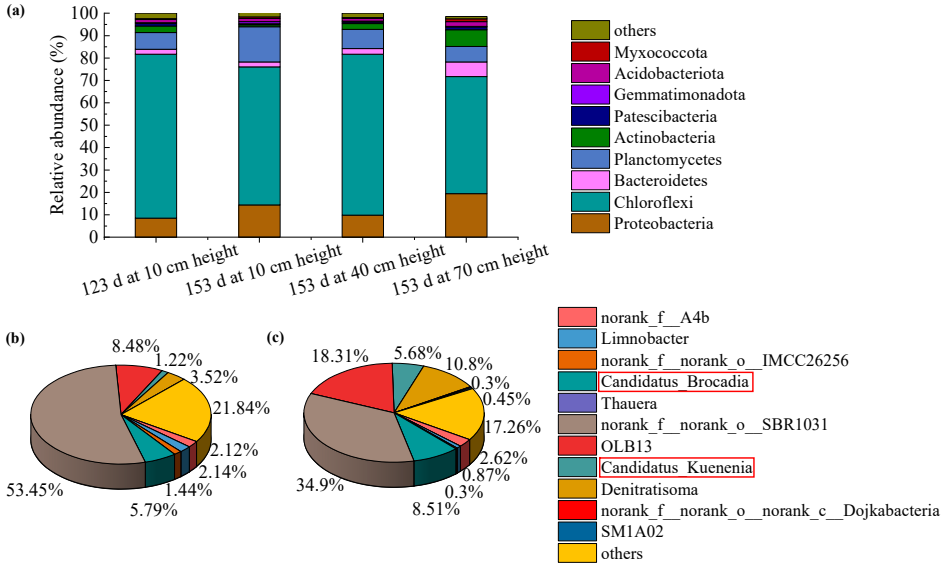

Figure 5. Microbial communities at the phylum level (**a**) and genus level (**b**,**c**) for UASB reactors operated for 123 d and 153 d. The red frame showed the functional bacteria of AnAOB.

The dominant bacteria at the genus level were *Denitratisoma* (3.51 and 10.8%) and *Candidatus brocadia* (5.77 and 8.51%) (Figure 5b). Among them, *Candidatus brocadia* is an anammox functional bacterium, and another anammox functional bacterium, *Candidatus kuenenia* (1.22 and 5.68%), was also detected. The relative abundance of both types of functional bacteria increased, indicating that the AnAOB in the system were gradually enriched with the operation of the reactor and the increase in influent load. The absence of ammonia-oxidizing bacteria in the samples may be related to the location where the sludge samples were taken. Apparently, the anammox system has the capacity to consume DO in the system, which may be absorbed close to the reactor inlet, while the samples were taken at 10 cm from the inlet. The heterotrophic bacteria *Denitratisoma* and *Limnobacter* were found in the system, and the minor presence of other microorganisms favored a system with some resistance to shocks such as organic loading. It has also been reported that the anammox system is achieved by the combined action of several microorganisms [51].

3.4. Effect of COD, NH_4^+-N and NO_2^--N on the Anammox Reaction in the Batch Test

Batch experiments on the inhibition of the anammox reaction by COD, NH_4^+-N, and NO_2^--N were conducted with the reactor sludge. Under initial NH_4^+-N and NO_2^--N concentrations of approximately 38 and 75 mg/L, respectively, the initial COD concentration increased from 0 to 800 mg/L, and the average conversion rate of NH_4^+-N decreased from

4.17 to 3.18 mg/(L·h), while the average conversion rate of NO_2^--N was in the range of 8.1–8.7 mg/L. NO_3^--N was not detected in the whole batch experiment (Table 2), which indicated that NO_3^--N was converted as soon as it was generated. The ΔNO_2^--N/ΔNH_4^+-N values during the reaction were all greater than the theoretical value of 1.32 [39] and increased with the initial COD concentration. This indicates that a small quantity of denitrification occurred in the system, and heterotrophic bacteria were found in the microbial community (Figure 5). The results suggest that high COD concentrations have a low inhibitory effect on the anammox reaction. However, long-term incubation in influent water containing organic matter may lead to the growth of heterotrophic bacteria in the system that compete with AnAOB for substrates [52,53]. Choi et al. showed that anammox inhibition was essentially absent or recovered within a day under transient organic loading (150 and 300 mg COD/L) shocks. Higher levels (≥60 mg COD/L) of continuous organic loading of influent water resulted in a significant decrease in anammox activity (complete inhibition at 150 mg COD/L) [53]. Chen et al. investigated the effect of C/N on the nitrogen removal effect of anammox and showed that the effluent deteriorated sharply when C/N increased to 1.31, and the nitrogen removal efficiency decreased to 49.2%. However, the microbial activity could be rapidly recovered when the organic inhibition was stopped [46]. Li et al. also showed that the presence of COD was harmful to anammox [54]. Fu et al. showed that when the influent TOC concentration was lower than 100 mg/L, the anammox activity was basically unaffected, and the maximum TN removal efficiency of the effluent reached 95.77%. However, when the influent TOC concentration reached 200 mg/L, the anammox reaction was severely inhibited, denitrification dominated, and the TN removal efficiency decreased to 64.17% [55]. In summary, higher concentrations of organics have an adverse effect on nitrogen removal efficiency, and if the influent water has a high concentration of organics, they should be removed before entering the anammox system.

Table 2. Effect of COD concentration on the anammox reaction.

Number	Initial COD Concentration	Initial NH_4^+-N Concentration	Initial NO_2^--N Concentration	Average Conversion Rate of NH_4^+-N	Average Conversion Rate of NO_2^--N	ΔNO_2^--N/ΔNH_4^+-N
	mg/L	mg/L	mg/L	mg/(L·h)	mg/(L·h)	
1	0	37.49 ± 3.2	71.16 ± 5.6	4.17 ± 0.5	8.18 ± 0.7	1.96 ± 0.2
2	50 ± 5	34.47 ± 3.2	76.26 ± 5.6	3.32 ± 0.5	8.58 ± 0.7	2.59 ± 0.2
3	100 ± 10	38.66 ± 3.2	75.26 ± 5.6	3.80 ± 0.5	8.61 ± 0.7	2.26 ± 0.2
4	500 ± 50	38.19 ± 3.2	74.72 ± 5.6	3.33 ± 0.5	8.30 ± 0.7	2.49 ± 0.2
5	800 ± 80	38.60 ± 3.2	75.97 ± 5.6	3.18 ± 0.5	8.65 ± 0.7	2.72 ± 0.2

The effect of NH_4^+-N on the anammox reaction was explored at initial NO_2^--N concentrations between 62.1 and 65.5 mg/L. As the initial NH_4^+-N concentration increased from 39.90 to 193.8 mg/L, the average NH_4^+-N conversion rate increased from 3.6 to 9.3 mg/(L·h) (Table 3). When the initial NH_4^+-N concentration was 210.7 mg/L, the NH_4^+-N conversion rate was reduced to 6.4 mg/(L·h), indicating that the conversion of NH_4^+-N was inhibited. However, at TN concentrations below 200 mg/L, the average NO_2^--N conversion rate increased from 7.3 to 7.5 mg/(L·h) with increasing NH_4^+-N concentration. When the TN concentration was greater than 200 mg/L, the NO_2^--N conversion rate decreased to 6.0 mg/(L·h), indicating that the conversion of nitrite was inhibited. Yang et al. similarly found an increase in effluent NH_4^+-N and NO_2^--N and a decrease in anammox activity after increasing influent total nitrogen [13]. Li et al. showed a high TN removal of 94.06 for influent NH_4^+-N and NO_2^--N, both greater than 100 mg/L. This was attributed to the incorporation of a pulsed electric field in the anammox system, which was apparently an effective method [54]. However, there were no extraneous substances in this study.

Table 3. Effect of initial NH_4^+-N concentration on the anammox reaction.

Number	Initial NH_4^+-N Concentration	Initial NO_2^--N Concentration	Initial TN Concentration	Average Conversion Rate of NH_4^+-N	Average Conversion Rate of NO_2^--N	ΔNO_2^--N/ΔNH_4^+-N
	mg/L	mg/L	mg/L	mg/(L·h)	mg/(L·h)	
1	39.90 ± 3.5	65.54 ± 5.2	105.4 ± 8.4	3.64 ± 0.3	7.28 ± 0.5	2.00 ± 0.1
2	87.14 ± 6.7	64.27 ± 5.2	151.4 ± 12.1	5.12 ± 0.4	7.34 ± 0.5	1.43 ± 0.1
3	127.7 ± 9.6	65.43 ± 5.2	193.1 ± 15.4	5.60 ± 0.4	7.45 ± 0.5	1.33 ± 0.1
4	193.8 ± 15.3	64.19 ± 5.2	258.0 ± 20.6	9.26 ± 0.5	6.99 ± 0.5	0.75 ± 0.1
5	210.7 ± 17.5	62.09 ± 5.2	272.8 ± 21.8	6.36 ± 0.4	5.91 ± 0.5	0.93 ± 0.1

The effect of NO_2^--N concentration on the anammox reaction was investigated when the initial NH_4^+-N concentration was between 33.1 and 35.0 mg/L. As the initial NO_2^--N concentration increased from 64.97 to 244.9 mg/L, the average NO_2^--N conversion rate increased from 7.1 to 12.1 mg/(L·h). However, the NO_2^--N conversion rate decreased to 10.9 mg/(L·h) when the nitrite concentration increased to 288.1 mg/L (Table 4). According to the TN results, the average conversion of NH_4^+-N increased with increasing initial NO_2^--N amount when the initial TN concentration was lower than 200 mg/L. In contrast, when the TN concentration was greater than 200 mg/L, the average conversion rate of NH_4^+-N decreased from 4.23 to 3.33 mg/(L·h). Batch experiments on the effect of both NH_4^+-N concentration and NO_2^--N concentration on anammox showed that the anammox reaction was inhibited when the TN concentration was greater than 200 mg/L. This is consistent with the conclusions obtained from the long-term operation of the reactor described above. Nitrite was previously reported to be the main cause of anammox inhibition, with irreversible inhibition caused when nitrite concentrations were increased above 100 mg/L [27,56]. The apparent inhibition in the present study appeared at NO_2^--N concentrations higher than 200 mg/L, which may be due to inconsistent culture conditions.

Table 4. Effect of initial NO_2^--N concentration on anammox reaction.

Number	Initial NH_4^+-N Concentration	Initial NO_2^--N Concentration	Initial TN Concentration	Average Conversion Rate of NH_4^+-N	Average Conversion Rate of NO_2^--N	ΔNO_2^--N/ΔNH_4^+-N
	mg/L	mg/L	mg/L	mg/(L·h)	mg/(L·h)	
1	33.75 ± 2.6	64.97 ± 5.2	98.72 ± 8.0	4.22 ± 0.3	7.14 ± 0.6	1.69 ± 0.2
2	34.96 ± 2.6	121.8 ± 9.7	156.7 ± 12.5	4.23 ± 0.3	10.79 ± 0.8	2.55 ± 0.2
3	33.62 ± 2.6	170.5 ± 13.6	204.2 ± 16.3	4.05 ± 0.3	11.48 ± 0.9	2.83 ± 0.2
4	33.81 ± 2.6	244.9 ± 19.6	277.7 ± 22.2	3.81 ± 0.2	12.07 ± 0.9	3.16 ± 0.2
5	33.12 ± 2.6	288.1 ± 23.0	319.2 ± 25.5	3.33 ± 0.2	10.85 ± 0.9	3.26 ± 0.2

Regarding the effect of initial NH_4^+-N in the experiment, the ΔNO_2^--N/ΔNH_4^+-N value decreased as NH_4^+-N increased and was lower than the theoretical value of 1.32 [39]. Regarding the batch tests on the effect of NO_2^--N, the ΔNO_2^--N/ΔNH_4^+-N values increased with increasing initial NO_2^--N concentration and were larger than the theoretical values. It is possible that the high concentration of substrate entering the system was easily and rapidly absorbed by microorganisms. To date, many studies have been conducted to reduce the inhibition of anammox bacteria through enrichment and to accelerate system start-up [14,57].

3.5. Discussion of Factors Influencing Anammox Enrichment

Anammox incubation conditions and influencing factors were explored based on long-term experimental data as well as batch experiments. AnAOB are considered sensitive to environmental conditions [43], and this study was conducted using a rough cultivation method. Anammox granular sludge was cocultured with conventional activated sludge

to accelerate AnAOB enrichment, and the microorganisms in the activated sludge were used to improve the resistance of AnAOB to adverse factors. In addition, the influent of the reactor contained 6–8 mg/L DO. The results showed that under both conditions, the activity of AnAOB was not significantly affected, and the reactor successfully started on 32 d. The maximum removal rate of TN was 81%, slightly lower than the theoretical value. The effective load of TN increased from 0.1 to 1.5 kg $N/m^3/d$ by increasing the influent volume. Notably, during long-term incubation from 63 to 81 d, the influent NH_4^+-N and NO_2^--N concentrations increased to 80 and 105.6 mg/L, and the influent TN was approximately 200 mg/L because the influent contained approximately 10 mg/L of NO_3^--N. Due to the inhibition caused by the substrate concentration [27,29], the nitrogen removal efficiency decreased, and the concentrations of effluent NH_4^+-N and NO_2^--N increased to 22 and 38 mg/L, respectively, with no decreasing trend. Subsequently, the influent concentration was reduced, the influent flow rate was increased, and the effluent NH_4^+-N and NO_2^--N remained below 5 mg/L. This indicates that when the substrate concentration is high enough to cause inhibition, AnAOB activity can be recovered if the influent water parameters are adjusted in a timely manner [29]. Batch tests further showed that the rate of nitrogen removal was affected at high substrate concentrations. In the existing research, the addition of exogenous substances (e.g., Fe, EPS, etc.) effectively solved the problems of substrate concentration inhibition and the slow rate of anammox [12,57,58]. However, inhibition of high-strength wastewater resulting in an increase in effluent concentration has not been addressed in this study. The addition of external substances is a major direction to solve this problem.

In this study, to address the difficulty of long generation times and slow cultivation of AnAOB, they were cocultured with waste sludge to accelerate their enrichment. There was no corresponding assessment of its contribution to the environment and resources. Sustainable assessment (e.g., full life cycle assessment) can be well realized to understand the environmental benefits of anammox technology and suggest ways to improve it [59]. Sustainability assessment is important for whether a technology is feasible for large-scale application. This is an essential direction for future research. Quorum sensing can provide insights into the effects of environmental quorums on the metabolic substrates of AnAOB [49,60]. Metabolomics and molecular modeling facilitate further insights into the biometabolic pathways of AnAOB during the enrichment process [61]. In the future, it is expected that the above techniques will be used to further understand the AnAOB enrichment process.

4. Conclusions and Prospects

Ordinary waste sludge and anammox granular sludge were mixed and inoculated in a 2:1 ratio, and rapid start-up and sludge enrichment in the anammox system were achieved with 6–8 mg/L DO in the influent water. Under an HRT of 2 h, the effluent NH_4^+-N was lower than 2 mg/L, the NO_2^--N was lower than 5 mg/L, the TN removal rate reached a maximum of 81%, and the TN load reached 1.5 kg $N/m^3/d$. The sludge EPS results showed that PN played a major role in the enrichment of anammox granular sludge, with PN/PS ranging from 5–6.3. Both SEM and high-throughput analyses indicated the presence of multiple types of microorganisms in the system. The anammox functional bacteria in the system were *Candidatus brocadia* and *Candidatus kuenenia*, with relative abundances of 8.51 and 5.68% on 153 d, respectively. TN concentrations above 200 mg/L inhibited the anammox reaction. In this case, it is possible to reduce the inhibition by adding foreign substances in the future. In this study, anammox granular sludge was used as the carrier to successfully convert ordinary flocculent sludge. This study was expected to solve the problem of insufficient anammox seed sludge, reduce the amount of anammox seed sludge and accelerate the enrichment of AnAOB. This study provides a new culture strategy for the use of the anammox process in large-scale wastewater treatment plants.

Supplementary Materials: The following supporting information can be downloaded at: https://www.mdpi.com/article/10.3390/su151612123/s1, Figure S1: The device sketch of UASB reactor; Figure S2: UASB reactor temperature and pH; Figure S3: ΔNO_2^--N/ΔNH_4^+-N and ΔNO_3^--N/ΔNH_4^+-N reacted in UASB reactor; Figure S4: 3D-EEM of different EPS compositions for UASB reactors: (a) and (b) LB-EPS on day 60 and day 130, respectively; (c) and (d) TB-EPS on day 60 and day 130, respectively.

Author Contributions: L.L.: Conceptualization, Methodology, Data curation, Writing—original draft; M.H.: Methodology, Investigation; C.W.: Data curation, Writing—original draft; W.Q.: Supervision, Writing—review and editing; Y.P.: Conceptualization. All authors have read and agreed to the published version of the manuscript.

Funding: This research was funded by National Natural Science Foundation of China (52000003 and 42277054); Key Research and Development Project of Shandong (2021CXGC011202 and 2022CXGC021002).

Institutional Review Board Statement: Not applicable.

Informed Consent Statement: Not applicable.

Data Availability Statement: The high-throughput original data are available at: https://submit.ncbi.nlm.nih.gov/subs/biosample/. BioProject ID: PRJNA980428.

Conflicts of Interest: The authors declare that they have no known competing financial interests or personal relationships that could have appeared to influence the work reported in this paper.

References

1. Li, J.; Peng, Y.; Zhang, L.; Gao, R.; Yang, L.; Liu, Q.; Zhang, Q.; Li, X.; Wang, S. Enhanced nitrogen removal assisted by mainstream partial-anammox from real sewage in a continuous flow A2/O reactor. *Chem. Eng. J.* **2020**, *400*, 125893. [CrossRef]
2. Cao, S.; Wang, S.; Peng, Y.; Wu, C.; Du, R.; Gong, L.; Ma, B. Achieving partial denitrification with sludge fermentation liquid as carbon source: The effect of seeding sludge. *Bioresour. Technol.* **2013**, *149*, 570–574. [CrossRef]
3. Dai, B.; Yang, Y.; Wang, Z.; Wang, J.; Yang, L.; Cai, X.; Wang, Z.; Xia, S. Enhancement and mechanisms of iron-assisted anammox process. *Sci. Total Environ.* **2023**, *858*, 159931. [CrossRef] [PubMed]
4. Cui, H.; Zhang, L.; Zhang, Q.; Li, X.; Peng, Y.; Wang, C. Enhancing nitrogen removal of carbon-limited municipal wastewater in step-feed biofilm batch reactor through integration of anammox. *Bioresour. Technol.* **2023**, *381*, 129091. [CrossRef] [PubMed]
5. Jetten, M.S.M.; Logemann, S.; Muyzer, G.; Robertson, L.A.; De Vries, S.; Van Loosdrecht, M.C.M.; Kuenen, J.G. Novel principles in the microbial conversion of nitrogen compounds. *Int. J. Gen. Mol. Microbiol.* **1997**, *71*, 75–93. [CrossRef]
6. Wang, J.; Zhang, S.; Li, J.; Yang, H. Municipal wastewater treatment via the two-stage partial nitrification-anammox (PN/A) process with gel immobilization. *J. Water Process Eng.* **2022**, *50*, 103267. [CrossRef]
7. Du, R.; Cao, S.; Niu, M.; Li, B.; Wang, S.; Peng, Y. Performance of partial-denitrification process providing nitrite for anammox in sequencing batch reactor (SBR) and upflow sludge blanket (USB) reactor. *Int. Biodeter. Biodegr.* **2017**, *122*, 38–46. [CrossRef]
8. Zhao, H.; Guo, Y.; Wang, Q.; Zhang, Z.; Wu, C.; Gao, M.; Liu, F. The Summary of Nitritation Process in Mainstream Wastewater Treatment. *Sustainability* **2022**, *14*, 16453. [CrossRef]
9. Yin, X.; Qiao, S.; Zhou, J.; Tang, X. Fast start-up of the anammox process with addition of reduced graphene oxides. *Chem. Eng. J.* **2016**, *283*, 160–166. [CrossRef]
10. Li, J.; Peng, Y.; Zhang, L.; Liu, J.; Wang, X.; Gao, R.; Pang, L.; Zhou, Y. Quantify the contribution of anammox for enhanced nitrogen removal through metagenomic analysis and mass balance in an anoxic moving bed biofilm reactor. *Water Res.* **2019**, *160*, 178–187. [CrossRef]
11. Huang, S.; Wu, D. Start-up Strategies for Anaerobic Ammonia Oxidation (Anammox) in In-Situ Nitrogen Removal from Polluted Groundwater in Rare Earth Mining Areas. *Sustainability* **2021**, *13*, 4591. [CrossRef]
12. Ma, M.; Cao, Q.; Mabruk, A.; Xie, J.; Wu, P.; Liu, W.; Chen, C. Promotion of nitrogen removal and microbial enrichment on anammox by exogenous substance addition: A critical review. *J. Water Process Eng.* **2022**, *49*, 103096. [CrossRef]
13. Yang, D.; Zuo, J.; Jiang, C.; Wang, D.; Gu, L.; Zhang, S.; Lu, H.; Wang, D.; Xu, S.; Bai, Z.; et al. Fast start-up of anammox process: Effects of extracellular polymeric substances addition on performance, granule properties, and bacterial community structure. *J. Environ. Manag.* **2023**, *338*, 117836. [CrossRef] [PubMed]
14. Tang, S.; Xu, Z.; Liu, Y.; Yang, G.; Mu, J.; Jin, R.; Yang, Q.; Zhang, X. Performance, kinetics characteristics and enhancement mechanisms in anammox process under Fe(II) enhanced conditions. *Biodegradation* **2020**, *31*, 223–234. [CrossRef]
15. Li, D.; Dang, Z.; Zhang, J. Study on two anammox start-up and operation strategies: Low-intensity direct current electric field and negative pressure. *Chem. Eng. J.* **2022**, *435*, 134791. [CrossRef]
16. Zekker, I.; Artemchuk, O.; Rikmann, E.; Ohimai, K.; Dhar Bhowmick, G.; Madhao Ghangrekar, M.; Burlakovs, J.; Tenno, T. Start-Up of Anammox SBR from Non-Specific Inoculum and Process Acceleration Methods by Hydrazine. *Water* **2021**, *13*, 350. [CrossRef]
17. Yuan, Q.; Jia, Z.; Roots, P.; Wells, G. A strategy for fast anammox biofilm formation under mainstream conditions. *Chemosphere* **2023**, *318*, 137955. [CrossRef]

18. Christensson, M.; Ekstrom, S.; Chan, A.A.; Le Vaillant, E.; Lemaire, R. Experience from start-ups of the first ANITA Mox Plants. *Water Sci. Technol.* **2013**, *67*, 2677–2684. [CrossRef]
19. Wang, Q.; Wang, Y.; Lin, J.; Tang, R.; Wang, W.; Zhan, X.; Hu, Z. Selection of seeding strategy for fast start-up of Anammox process with low concentration of Anammox sludge inoculum. *Bioresour. Technol.* **2018**, *268*, 638–647. [CrossRef]
20. Liu, Q.; Li, J.; Zhao, Y.; Li, X.; Zhang, Q.; Sui, J.; Wang, C.; Peng, Y. Mechanism of suspended sludge impact on anammox enrichment in anoxic biofilm through long term operation and microbial analysis. *Water Res.* **2023**, *229*, 119412. [CrossRef]
21. Lotti, T.; Kleerebezem, R.; Lubello, C.; van Loosdrecht, M.C.M. Physiological and kinetic characterization of a suspended cell anammox culture. *Water Res.* **2014**, *60*, 1–14. [CrossRef] [PubMed]
22. Zhao, Q.; Li, J.; Deng, L.; Jia, T.; Zhao, Y.; Li, X.; Peng, Y. From hybrid process to pure biofilm anammox process: Suspended sludge biomass management contributing to high-level anammox enrichment in biofilms. *Water Res.* **2023**, *236*, 119959. [CrossRef] [PubMed]
23. Tao, Y.; Gao, D.; Wang, H.; de Kreuk, M.; Ren, N. Ecological characteristics of seeding sludge triggering a prompt start-up of anammox. *Bioresour. Technol.* **2013**, *133*, 475–481. [CrossRef]
24. Egli, K.; Fanger, U.; Alvarez, P.J.J.; Siegrist, H.; van der Meer, J.R.; Zehnder, A.J.B. Enrichment and characterization of an anammox bacterium from a rotating biological contactor treating ammonium-rich leachate. *Arch. Microbiol.* **2001**, *175*, 198–207. [CrossRef]
25. Geng, L.; Yang, H.; Wang, X.; Liu, X.; Wang, J.; Su, Y. Inhibition and recovery of ANAMMOX with Na2SO3: From performance to microbial community analysis. *J. Environ. Chem. Eng.* **2023**, *11*, 109051. [CrossRef]
26. Hu, M.; Liu, X.; Ya, T.; Liu, J.; Zhang, M.; Wang, X. Dissolved oxygen alters the microbial interactions of anammox consortia in PN/A process. *J. Water Process Eng.* **2023**, *53*, 103697. [CrossRef]
27. Chen, H.; Cao, S.; Chen, L.; Zhang, Z.; Tian, J.; Jin, R.; Yao, J. Biochar accelerates the start-up of the anammox process: Phenomenon and potential mechanisms. *J. Water Process Eng.* **2023**, *53*, 103662. [CrossRef]
28. Wang, T.; Zhang, D.; Sun, Y.; Zhou, S.; Li, L.; Shao, J. Using low frequency and intensity ultrasound to enhance start-up and operation performance of Anammox process inoculated with the conventional sludge. *Ultrason. Sonochem.* **2018**, *42*, 283–292. [CrossRef]
29. Wang, S.; Guo, J.; Lian, J.; Ngo, H.H.; Guo, W.; Liu, Y.; Song, Y. Rapid start-up of the anammox process by denitrifying granular sludge and the mechanism of the anammox electron transport chain. *Biochem. Eng. J.* **2016**, *115*, 101–107. [CrossRef]
30. Tang, C.; Zheng, P.; Chai, L.; Min, X. Characterization and quantification of anammox start-up in UASB reactors seeded with conventional activated sludge. *Int. Biodeter. Biodegr.* **2013**, *82*, 141–148. [CrossRef]
31. Bi, Z.; Qiao, S.; Zhou, J.; Tang, X.; Zhang, J. Fast start-up of Anammox process with appropriate ferrous iron concentration. *Bioresour. Technol.* **2014**, *170*, 506–512. [CrossRef] [PubMed]
32. Wang, T.; Liu, Y.; Guo, J.; Song, Y.; Gu, J.; Lian, J.; Lu, C.; Han, Y.; Li, H.; Hou, Y. Rapid start up anammox process through a new strategy with inoculating perchlorate reduction sludge and a small amount of anammox sludge. *Biochem. Eng. J.* **2020**, *164*, 107784. [CrossRef]
33. He, X.; Shi, S.; Huang, W.; Fan, X.; Zhou, J.; Chen, Y.; Wang, Y. A novel Electrolysis-integrated anammox system for intensified nitrogen removal and simultaneous phosphorus recovery as vivianite. *Chem. Eng. J.* **2023**, *466*, 143299. [CrossRef]
34. Zheng, Y.; Zhao, Y.; Su, R.; An, N.; Zhang, Y.; Wei, Y.; Ma, B. A novel method for immobilizing anammox bacteria in polyurethane foam carriers through dewatering. *J. Water Process Eng.* **2023**, *53*, 103738. [CrossRef]
35. Qi, W.; Liu, L.; Shi, Q.; Su, X.; Lv, Q.; Peng, Y.; Wang, C. Process research of one-stage partial nitrification-anammox (S-PN/A) technology in toilet water treatment and related kinetic simulation. *J. Chem. Technol. Biotechnol.* **2021**, *96*, 3414–3425. [CrossRef]
36. Du, R.; Cao, S.; Zhang, H.; Peng, Y. Formation of partial-denitrification (PD) granular sludge from low-strength nitrate wastewater: The influence of loading rates. *J. Hazard. Mater.* **2020**, *384*, 121273. [CrossRef] [PubMed]
37. Wan, K.; Yu, Y.; Hu, J.; Liu, X.; Deng, X.; Yu, J.; Chi, R.; Xiao, C. Recovery of anammox process performance after substrate inhibition: Reactor performance, sludge morphology, and microbial community. *Bioresour. Technol.* **2022**, *357*, 127351. [CrossRef] [PubMed]
38. Chang, G.; Yang, Y.; Yang, Y.; Yang, J.; Li, S.; Mu, X.; Luo, J.; Li, X. Alleviation of substrate inhibition in an anaerobic ammonia oxidation reactor: Recovery process performance and microbial community. *J. Water Process Eng.* **2023**, *51*, 103439. [CrossRef]
39. Kuenen, J.G. Anammox bacteria: From discovery to application. *Nat. Rev. Microbiol.* **2008**, *6*, 320–326. [CrossRef]
40. Du, R.; Cao, S.; Li, X.; Wang, J.; Peng, Y. Efficient partial-denitrification/anammox (PD/A) process through gas-mixing strategy: System evaluation and microbial analysis. *Bioresour. Technol.* **2020**, *300*, 122675. [CrossRef]
41. Qiao, X.; Fu, C.; Chen, Y.; Fang, F.; Zhang, Y.; Ding, L.; Yang, K.; Pan, B.; Xu, N.; Yu, K.; et al. Molecular insights into enhanced nitrogen removal induced by trace fluoroquinolone antibiotics in an anammox system. *Bioresour. Technol.* **2023**, *374*, 128784. [CrossRef]
42. Zhang, Q.; Zheng, J.; Zhao, L.; Liu, W.; Chen, L.; Cai, T.; Ji, X. Succession of microbial communities reveals the inevitability of anammox core in the development of anammox processes. *Bioresour. Technol.* **2023**, *371*, 128645. [CrossRef]
43. Hou, X.; Liu, S.; Zhang, Z. Role of extracellular polymeric substance in determining the high aggregation ability of anammox sludge. *Water Res.* **2015**, *75*, 51–62. [CrossRef]
44. Xue, Y.; Liu, X.; Dang, Y.; Shi, T.; Sun, D. Enhancement of nitrogen removal in coupling Anammox and DAMO via Fe-modified granular activated carbon. *J. Environ. Manag.* **2023**, *340*, 118001. [CrossRef] [PubMed]

45. Chen, W.; Westerhoff, P.; Leenheer, J.A.; Booksh, K. Fluorescence Excitation−Emission Matrix Regional Integration to Quantify Spectra for Dissolved Organic Matter. *Environ. Sci. Technol.* **2003**, *37*, 5701–5710. [CrossRef]
46. Chen, H.; Liu, G.; Zhu, J.; Ma, X.; Piao, C.; Li, X.; Wang, K. Investigation of the mechanism of anammox granules alleviating the inhibition of organic matter in pharmaceutical wastewater. *J. Clean. Prod.* **2023**, *398*, 136129. [CrossRef]
47. Fan, W.; Chen, Y.; Yuan, B.; Chen, X.; Wang, Q.; Zhao, S.; Jia, W. Enhancing anammox nitrogen removal by static magnetic field exposure: Performance, microbial community and symbiotic relationship analysis. *J. Water Process Eng.* **2023**, *53*, 103709. [CrossRef]
48. Zhao, Y.; Liu, S.; Jiang, B.; Feng, Y.; Zhu, T.; Tao, H.; Tang, X.; Liu, S. Genome-Centered Metagenomics Analysis Reveals the Symbiotic Organisms Possessing Ability to Cross-Feed with Anammox Bacteria in Anammox Consortia. *Environ. Sci. Technol.* **2018**, *52*, 11285–11296. [CrossRef]
49. Gao, M.; Zou, X.; Dang, H.; Mohammed, A.N.; Yang, S.; Zhou, Y.; Yao, Y.; Guo, H.; Liu, Y. Exploring interactions between quorum sensing communication and microbial development in anammox membrane bioreactor. *J. Environ. Chem. Eng.* **2023**, *11*, 109339. [CrossRef]
50. Kindaichi, T.; Yuri, S.; Ozaki, N.; Ohashi, A. Ecophysiological role and function of uncultured Chloroflexi in an anammox reactor. *Water Sci. Technol.* **2012**, *66*, 2556–2561. [CrossRef]
51. Ya, T.; Du, S.; Li, Z.; Liu, S.; Zhu, M.; Liu, X.; Jing, Z.; Hai, R.; Wang, X. Successional Dynamics of Molecular Ecological Network of Anammox Microbial Communities under Elevated Salinity. *Water Res.* **2021**, *188*, 116540. [CrossRef] [PubMed]
52. Daigger, G.T. Oxygen and Carbon Requirements for Biological Nitrogen Removal Processes Accomplishing Nitrification, Nitritation, and Anammox. *Water Environ. Res.* **2014**, *86*, 204–209. [CrossRef] [PubMed]
53. Choi, H.; Kim, J.; Park, J.; Lee, C. Response of granular anammox process under mainstream conditions to continuous and transient organic loads. *Chem. Eng. J.* **2023**, *464*, 142681. [CrossRef]
54. Li, L.; Bian, D.; Wang, Q.; Xue, C.; Zhang, Q.; Zhang, S.M. Performance of anammox enchanced by pulsed electric fields under added organic carbon sources using integrated network and metagenomics analyses. *Bioresour. Technol.* **2023**, *380*, 129116. [CrossRef]
55. Fu, W.; Zhu, R.; Lin, H.; Zheng, Y.; Hu, Z. Effect of organic concentration on biological activity and nitrogen removal performance in an anammox biofilm system. *Water Sci. Technol.* **2021**, *84*, 725–736. [CrossRef] [PubMed]
56. Strous, M.; Kuenen, J.G.; Jetten, M.S.M. Key Physiology of Anaerobic Ammonium Oxidation. *Appl. Environ. Microb.* **1999**, *65*, 3248–3250. [CrossRef]
57. Zhang, Q.; Feng, Z.; Zhou, J.; Ma, X.; Sun, Y.; Liu, J.; Zhao, J.; Jin, R. Roles of Fe(II), Fe(III) and Fe0 in denitrification and anammox process: Mechanisms, advances and perspectives. *J. Water Process Eng.* **2023**, *53*, 103746. [CrossRef]
58. Wang, Z.; Liu, X.; Ni, S.; Zhuang, X.; Lee, T. Nano zero-valent iron improves anammox activity by promoting the activity of quorum sensing system. *Water Res.* **2021**, *202*, 117491. [CrossRef]
59. Hao, X.; Wang, X.; Liu, R.; Li, S.; van Loosdrecht, M.C.M.; Jiang, H. Environmental impacts of resource recovery from wastewater treatment plants. *Water Res.* **2019**, *160*, 268–277. [CrossRef]
60. Chen, X.; Liu, L.; Bi, Y.; Meng, F.; Wang, D.; Qiu, C.; Yu, J.; Wang, S. A review of anammox metabolic response to environmental factors: Characteristics and mechanisms. *Environ. Res.* **2023**, *223*, 115464. [CrossRef]
61. Huang, D.; Wang, Y.; Li, Z.; Huang, B.; Yang, M.; Fan, N.; Jin, R. Metabolomics and molecular simulation reveal the responding mechanism of anammox consortia to perfluorooctanoic acid by regulating metabolic network. *Chem. Eng. J.* **2023**, *460*, 141712. [CrossRef]